Size Effect on Diagonal Shear Failure of Beams without Stirrups

by Zdeněk P. Bažant and Mohammad T. Kazemi

Presents the results of recent tests on diagonal shear failure of reinforced concrete beams without stirrups. The beams are geometrically similar, and the size range is 1:16. The test results indicate a significant size effect and show a good agreement with Bažant's law for size effect. Scatter of the test results is much lower than that previously found by studying extensive test data from the literature, which have not been obtained on geometrically similar beams. The tests also show that preventing bond slip of the longitudinal bars (by providing end anchorage with hooks) causes an increase of the brittleness number of the beam. It is concluded that the current design approach, which is intended to provide safety against the diagonal crack initiation load, should be replaced or supplemented by a design approach based on the ultimate load, in which a size effect of the fracture mechanics type, due to release of stored energy, must be taken into account. A relatively simple adjustment of the existing formula might be sufficient for design, although determination of the brittleness number of the beam deserves more study.

The diagonal shear failure of reinforced concrete beams has long been known to be a brittle type of failure. As a consequence, a larger safety margin is provided by the capacity-reduction factor in the codes. However, all the consequences of brittleness have not been fully appreciated. Brittleness also necessarily implies the existence of size effect on the failure load, which is due to the release of stored elastic energy and the progressive nature of failure. This aspect of brittleness has so far been neglected by design codes.

The present code formulas have been calibrated to provide adequate safety against the initiation of diagonal shear cracks. However, the crack initiation load is not proportional to the ultimate (maximum) load. It can be much smaller, or only slightly smaller,[1] depending on beam size and other factors. Therefore, the existing design formulas cannot be expected to provide a uniform safety margin against failure. Ideally, the design should insure proper safety margins against both: (1) failure, and (2) crack initiation. The first criterion is certainly the most important if preventing catastrophic collapse is the primary objective of design.

Several studies[2-4] have recently addressed the size effect, exploiting the test data that exist in the literature (see the survey of data sets in Reference 4). These analyses confirmed the theoretical prediction that there is indeed a significant size effect, but did not confirm the precise form of the size-effect law, because the scatter of the data was too large. The excessive scatter occurred because the previous tests were not carried out with geometrically similar beams and the size ranges tested were insufficiently broad. The lack of similarity required adjustments to be made according to known approximate formulas for the effect of other factors, like shear span, which involve additional errors that have nothing to do with the size effect and thus obscure the size effect. So the need for further tests satisfying geometrical similarity conditions became apparent. The purpose of this paper is to report the results of such tests and identify from them the size effect more clearly.

REVIEW OF SIZE-EFFECT LAW
The size effect is defined by comparing geometrically similar specimens or structures of different sizes. The ultimate load (maximum load) P_u is characterized by the nominal stress at failure

$$\sigma_N = c_n \frac{P_u}{bd} \qquad (1)$$

in which b = thickness of the structure (in the case of two-dimensionally similar structures), d = characteris-

Zdeněk P. Bažant, FACI, is Walter P. Murphy Professor of Civil Engineering at Northwestern University, Evanston, Ill., where he served as founding Director of the Center for Concrete and Geomaterials. He is a registered structural engineer, a consultant to Argonne National Laboratory, and editor-in-chief of the ASCE Journal of Engineering Mechanics. He is chairman of ACI Committee 446, Fracture Mechanics; a member of ACI Committees 209, Creep and Shrinkage of Concrete, and 348, Structural Safety; chairman of RILEM Committee TC 107 on Creep, of ASCE-EMD Programs Committee, and of SMiRT Division of Concrete and Nonmetallic Materials; and a member of the Board of Directors of the Society of Engineering Science. Currently he conducts research at the Technical University in Munich under the Humboldt Award of U.S Senior Scientist.

Mohammad T. Kazemi holds a PhD in structural engineering from Northwestern University. He holds MS and BS degrees from Sharif University of Technology, Tehran. His current research interests includes fracture mechanics of concrete and other quasi-brittle materials. He is a faculty member at Sharif University.

tic dimension of the structure, and c_n = coefficient introduced for convenience. It does not matter which dimension of the structure is used for d because only relative values are of interest; e.g., one can use the beam depth, beam span, or shear span. Coefficient c_n can be defined to make σ_N represent the maximum bending stress in the beam, or the average shear stress, or any other convenient stress value.

When geometrically similar structures of different sizes fail at the same σ_N, we say that there is no size effect. It can be verified that size effect is not exhibited by plastic limit analysis, nor by elastic analysis with an allowable stress criterion, nor any failure criterion based on a failure surface in the stress space or the strain space. This means that σ_N = constant = Bf_u obtained from plastic limit analysis (B = nondimensional constant and f_u = any measure of strength, also a constant). The absence of size effect is due to the fact that the failure is, according to plasticity, always simultaneous throughout the structure, occurring as a single-degree-of-freedom mechanism. Fracture mechanics, on the other hand, deals with failures which are nonsimultaneous, i.e., propagating. The propagation nature of failure gives rise to size effect, unless the failure occurs (or is assumed to occur) at the first initiation of fracture. According to linear elastic fracture mechanics — the simplest fracture theory in which the fracture process is assumed to be concentrated at a point (the crack tip) — one must always have σ_N = (const.)$xd^{-1/2}$, which represents the strongest possible size effect. Applicability of such a size effect to diagonal shear was first analyzed in a pioneering study of Reinhardt,[5] who initiated study of the problem from the fracture mechanics viewpoint.

For propagating failures in which the fracture process is not concentrated at a point, but takes place within a finite zone ahead of the fracture front, the size effect is transitional between plasticity and linear elastic fracture mechanics. A transitional size effect may be simply described by the law proposed by Bažant[6]

$$\sigma_N = Bf_u (1 + \beta)^{-1/2}, \qquad \beta = d/d_0 \qquad (2)$$

in which d_0 and B are empirical constants and ratio β is called the brittleness number[7] (which must be distinguished from the brittleness numbers of Gustafsson and Hillerborg[8] and Carpinteri[9]).

Eq. (2) has been rigorously derived from various reasonable simplifying hypotheses. It can be derived[6] by dimensional analysis and similitude arguments from the hypothesis that the dissipated energy depends on: (1) length of the fracture of cracking zone and (2) its area. If only the first part of the hypothesis is made, the size effect of linear elastic fracture mechanics results, and if only the second part of the hypothesis is made, there is no size effect, as in plasticity. Eq. (2) also results from fracture mechanics when the fracture process zone ahead of a sharp crack tip is assumed to have a certain constant length which is a material property and is independent of the structure size.

It must be emphasized that Eq. (2) is approximate. However (in comparison with the inevitable statistical scatter in concrete testing), the accuracy is sufficient for size ranges up to 1:20, which is good enough for most practical purposes. More complicated formulas for a broader range of applicability have been considered;[7,10] however, the additional parameters were found not to be independent of the structure shape, while Eq. (2) seems to work well for any reasonable specimen or structure shape tested so far.

In the case of structures that have no notches, applicability of Eq. (2) rests on the assumption that the ultimate load is not reached at the first initiation of cracking or damage, but is reached only after a large damage, or fracture zone, or both, develops. In fact, a good design practice requires concrete structures to be designed so that the ultimate load will be much larger than the first cracking load, and this guarantees the existence of a large cracking or damage zone at the moment of failure. This zone has a similar effect as a large fracture or notch, causing stress redistribution with stress concentrations at the fracture or damage front.

Applicability of Eq. (2) to structures also requires that the shape of the major crack and the contour of the cracking zone at ultimate load, observed on specimens of different sizes, be approximately similar. It may happen that Eq. (2) works only up to a certain size, beyond which this condition is no longer satisfied and a transition to a different failure mechanism takes place (such a limit of applicability has, for example, been found for the case of Brazilian split-cylinder tests).

TEST SPECIMENS AND PROCEDURE

Two different test series with effective beam depths d as given in Table 1 have been carried out (d = distance from the compression face to the centroid of tensile reinforcement). In the first series, with sizes in the ratio 1:2:4:8, the longitudinal reinforcing bars were straight, while in the second series, with sizes in the ratio 1:2:4:8:16, the reinforcing bars were provided with right-angled hooks at the beam ends to prevent bond slip and bar pullout at failure. In the smallest specimens of the first series, pullout failures with bond slip were observed, causing the failure mechanism to change
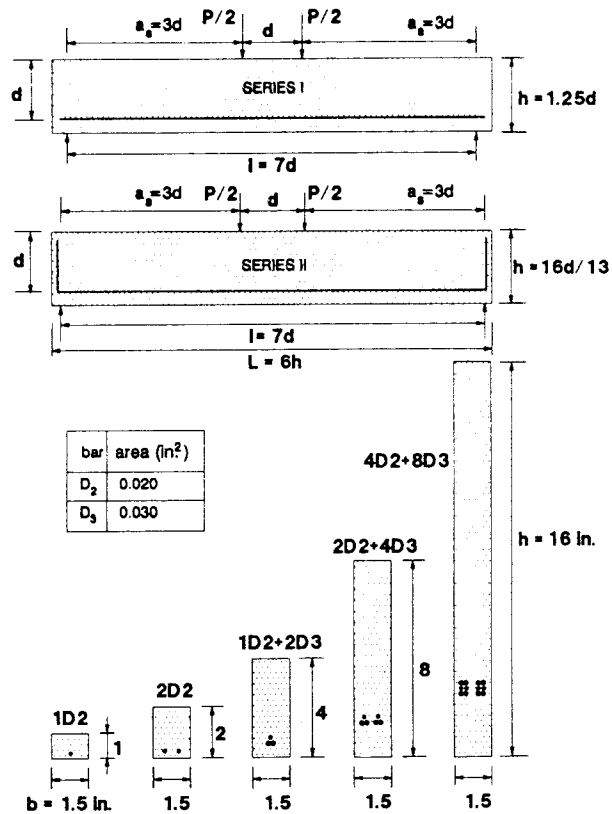
Fig. 1—Test-specimen geometry (1 in. = 25.4 mm)

Table 1 — Results of diagonal shear tests at Northwestern University

(I) Unanchored bars (f'_c = 6790 psi)				(II) Anchored bars (f'_c = 6700 psi)			
d, in.	P_u, kips	$\frac{v_u}{v_c}$	Observed failure mode	d, in.	P_u, kips	$\frac{v_u}{v_c}$	Observed failure mode
0.8	0.65 0.66 0.71	1.53 1.55 1.67	Bar pullout and bending	13/16	0.94 1.09 1.05	2.19 2.54 2.45	Diagonal shear and bending
1.6	1.46 1.33 1.39	1.72 1.56 1.63		1.625	1.32 1.21 1.43	1.54 1.41 1.67	
3.2	2.47 2.51 2.33	1.45 1.48 1.37	Diagonal shear (single main peak, failure at one side only)	3.25	2.43 2.26 2.00	1.42 1.32 1.17	Diagonal shear (single main peak, failure at one side only)
6.4	4.08	1.20		6.5	3.28 (3.76)	0.96 —	Diagonal shear (two peaks, major cracks at both sides)
	4.40 (4.63)	1.29 —	Diagonal shear (two peaks)		3.77 (5.44)	1.10 —	
	4.56	1.34	Diagonal shear (single peak)		3.69	1.08	
Not tested				13.0	4.62 5.06 4.16	0.67 0.74 0.61	Diagonal shear (single main peak)

1 in. = 25.4 mm, 1 kip = 1000 lb = 4448 N, 1 psi = 6895 Pa.
$v_u = \sigma_N = P_u/2bd$, v_c = 1.222 and 1.212 MPa (177.2 and 175.8 psi) for the first and second series, respectively [see Eq. (3)].

at least partially from diagonal shear to bending. The length-to-height ratio of all the beams was $L/h = 6$, and the span-to-depth ratio was $\ell/d = 7$. The loads were positioned so that the shear span was always $a_s = 3d$ (see Fig. 1) and the total cross-sectional height $h = 5d/4$ and $16d/13$ for the first and second series, respectively.

The thickness of all the specimens was $b = 38.1$ mm (1.5 in.). In the present tests, because the same thickness was kept for all sizes, the largest beams had a rather thin and slender (elongated) cross section. Nevertheless, the slenderness of the cross section was much below the critical value for which lateral buckling would take place.

It may be proper to cite the reasons for the beam thickness to be kept constant (two-dimensional similarity) rather than increased in proportion to the beam depth (three-dimensional similarity).

1. The surface layer of concrete, of a thickness roughly equal to the maximum aggregate size, has, inevitably, a considerably smaller content of large aggregate pieces and a considerably larger content of mortar. This phenomenon, called the "wall effect," is known to cause the fracture front to advance on the surface farther than in the interior, and may be expected to cause the thickness average of the fracture energy to vary as the thickness increases.

2. The midthickness of the specimen is roughly in the state of plane strain and the surface layer is approximately in the state of plane stress, which also causes the

fracture energy to be different near the specimen surface than it is in the interior. The average fracture energy thus can be kept constant only if the specimen thickness is constant.

3. According to linear elastic fracture mechanics, the Poisson effect causes the singularity at the surface termination of the crack front edge to be different from that in the interior. The effect of this difference must diminish if the thickness increases.

4. When the specimen thickness is varied, additional size effects are produced by diffusion phenomena such as heat conduction and drying; for example, hydration heat causes the core of a thicker specimen to heat to higher temperatures than does the core of a thinner specimen, which affects the development of strength as well as damage.

5. Changes of thickness might also cause a Weibull-type statistical size effect.

Despite these theoretical reasons, however, no significant effect of thickness on the diagonal shear strength has been observed in tests within a realistic thickness range.[11]

The longitudinal reinforcing bars used for both test series were cold-drawn deformed steel bars with strength 690 to 890 MPa (100 to 130 ksi). Because of difficulties in obtaining bars of geometrically similar cross sections, it was decided to make only the cross-sectional areas geometrically similar and use for all the specimens various combinations of bar sizes D2 and D3 whose effective areas are 12.90 and 19.75 mm² (0.020 and 0.030 in.²), respectively. The bar locations and size combinations used for various specimen sizes are shown in Fig. 1, for both test series. The reinforcement ratios, $\rho = A_s/bd$, were 1.65 and 1.62 percent for the first and second series, respectively (A_s = cross-sectional area of reinforcement).

270

A microconcrete was used (for reasons of economy), with maximum aggregate size 4.8 mm (3/16 in.), essentially the same as that used by Bažant and Pfeiffer.[10] The water:cement:aggregate ratio was 1:2:4 (by weight). The compression strength of concrete f'_c was 46.8 and 46.2 MPa (6.79 and 6.70 ksi) for the first and second series, respectively, as measured on cylinders 76 mm (3 in.) in diameter and 152 mm (6 in.) high. Neither admixtures nor air-entraining agents were used. Mineralogically, the aggregate was siliceous river sand. Portland cement C 150 (ASTM Type I) was used.

All the beams were cast in plywood forms. The forms were stripped at 1 day of age. Subsequently, the specimens were cured until the day of the test at 95 percent relative humidity and with a temperature at approximately 25 C. To reduce errors in comparing beams of different sizes, each whole series of beams of all sizes was cast from a single batch of concrete. For the same reasons, the specimens were all cured side by side.

The specimens were tested at the age of 28 days in a closed-loop MTS machine under constant stroke rate, which was chosen to achieve the maximum load for each size within about 7 min.

TEST RESULTS AND THEIR EVALUATION

The measured values of maximum (ultimate) loads for the individual specimens are given in Table 1, which also reports the nominal stresses at maximum load, $v_u = \sigma_N = P_u/2bd$, as normalized by v_c [see Eq. (3)] ($c_n = 1/2$, which means σ_N is chosen to represent the average shear stress).

The observed types of failure are also indicated in Table 1. In most cases, the failure was of the diagonal shear type, as planned. However, for the smallest specimens of the first series, failure occurred essentially by bending combined with pullout of the bars from the end parts of the beams; therefore, these results were not used in the analysis. In the second series, the pullout was prevented by right-angled hooks. But the failure of the smallest specimens was still not entirely of the diagonal shear type; rather, the cracking pattern of these specimens appeared as a combination of diagonal shear and bending, while for all the larger specimens it appeared as typical diagonal shear.

In most cases, one main diagonal crack, at one side of the beam, developed during failure (maximum load) and the secondary peak due to the diagonal crack at the other side (if registered) was smaller. However, in a few instances (indicated in Table 1), the overall maximum load corresponded to the second large diagonal crack. In those cases, a major crack developed first at one side but was later arrested at the compression zone; after that the load dropped, but started to rise again as another large crack developed at the other side. During the growth of the second large crack, a higher peak load was reached. Only the first of the two main peak loads agreed reasonably well with the overall trend of the size effect, and was therefore considered in the analysis given in Table 1. It would in any case be unreasonable to design a beam for the second main peak,
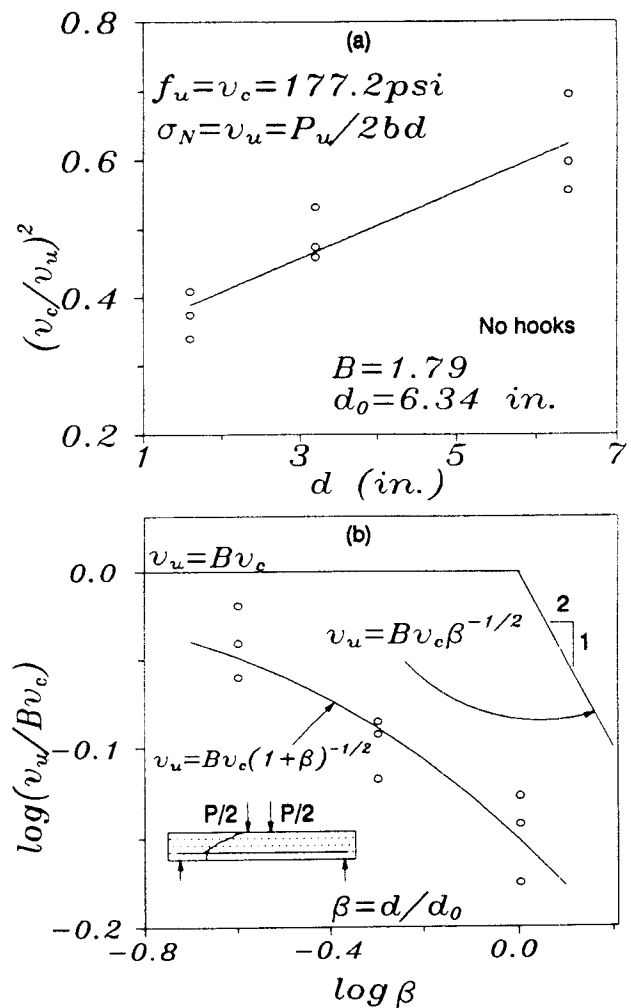
Fig. 2—Size-effect plots for the first series and size range 2:8 (1 in. = 25.4 mm, 1 psi = 6895 Pa)

regardless of which main peak is higher. In practice, the peak-load state due to the first large diagonal shear crack must be considered to be catastrophic failure. The failure mode at this state is the same as that for the majority of the beams tested, for which a large diagonal crack developed only at one side under the maximum load. This occurred in the first series for one and in the second series for two specimens, all with height $h = 203$ mm (8 in.).

ANALYSIS OF TEST RESULTS

The constants in Eq. (2) can be conveniently determined by linear regression, since the advantage of Eq. (2) is that it can be rearranged to a linear plot $Y = AX + C$, with $X = d$, $Y = (f_u/\sigma_N)^2 = (v_c/v_u)^2$, $A = C/d_0$, and $C = B^{-2}$. Thus, plotting Y versus X, and determining the slope and vertical intercept of the regression line, one obtains d_0 and B.

These regression plots are shown in Fig. 2(a) and 3(a), which also give the resulting optimal values of d_0 and B. From this, the size-effect curve may be plotted in the form of logarithm of the nominal stress versus the logarithm of the brittleness number, which is a measure of size. Such plots are shown for both series in
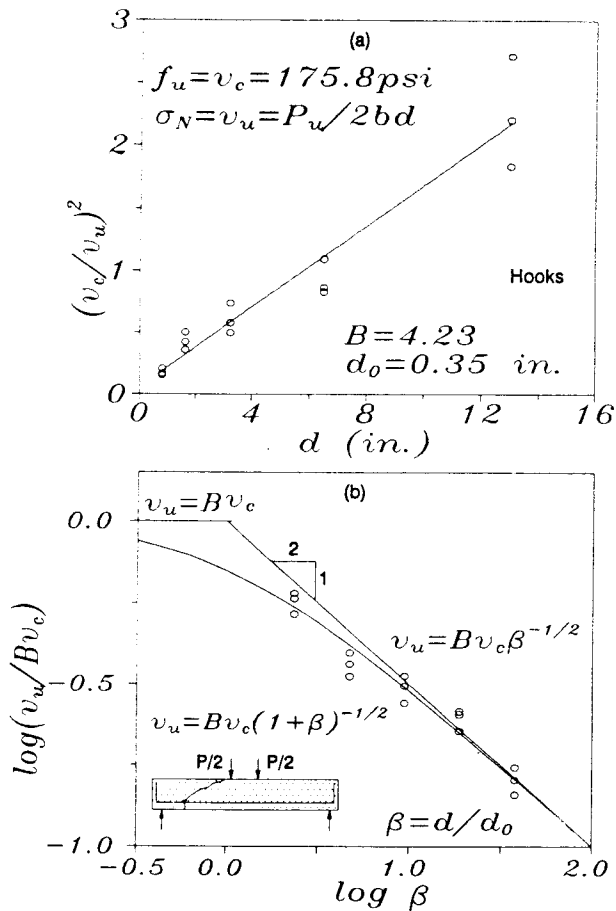
(a)

$f_u = v_c = 175.8\,psi$

$\sigma_N = v_u = P_u/2bd$

$(v_c/v_u)^2$

Hooks

$B = 4.23$
$d_0 = 0.35\ in.$

$d\ (in.)$

(b)

$v_u = B v_c$

$v_u = B v_c \beta^{-1/2}$

$v_u = B v_c (1+\beta)^{-1/2}$

$\beta = d/d_0$

$log(v_u/Bv_c)$

$log\ \beta$

Fig. 3—Size-effect plots for the second series and entire size range, 1:16 (1 in. = 25.4 mm, 1 psi = 6895 Pa)

$v_u = B v_c$

$v_c = 175.8\ psi$

$B = 3.93$
$d_0 = 0.40\ in.$

$v_u = B v_c \beta^{-1/2}$

$v_u = B v_c (1+\beta)^{-1/2}$

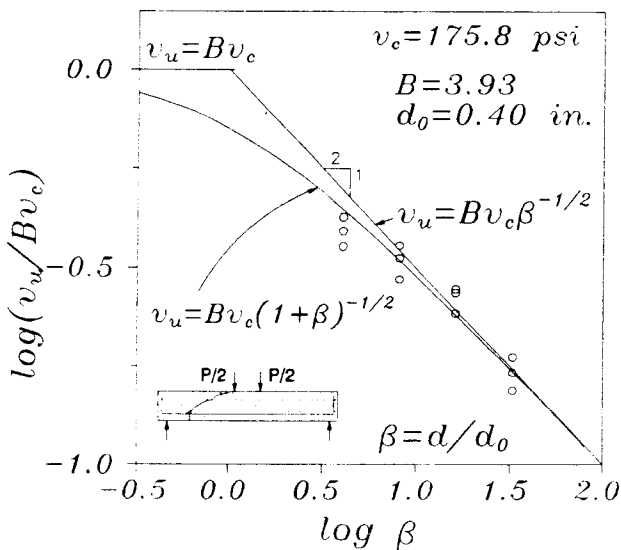$\beta = d/d_0$

$log(v_u/Bv_c)$

$log\ \beta$

Fig. 4—Size-effect plot for the second series without the smallest size; size range 2:16 (1 in. = 25.4 mm, 1 psi = 6895 Pa)

Fig. 2(b) and 3(b). The size effect according to linear elastic fracture mechanics is in these plots represented by a straight line of slope $-1/2$, as shown. This straight line represents the asymptote of the size-effect curve for $\beta \to \infty$.

$v_u = B v_c$

$B = 1.95$
$d_0 = 2.59\ in.$

$v_u = B v_c \beta^{-1/2}$

$v_u = B v_c (1+\beta)^{-1/2}$

$v_c = 175.8\ psi$
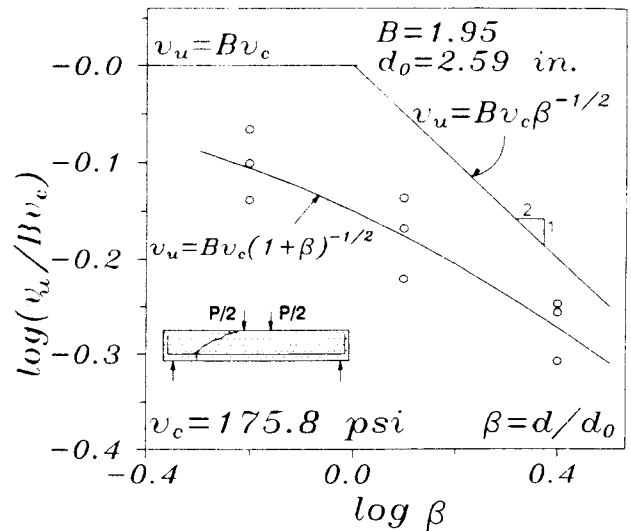
$\beta = d/d_0$

$log(v_u/Bv_c)$

$log\ \beta$

Fig. 5—Size-effect plot for the second series without the smallest and largest sizes; size range 2:8 (1 in. = 25.4 mm, 1 psi = 6895 Pa)

It is interesting to note that for the first series the results were relatively far from the linear elastic fracture mechanics asymptote and for the second series they were very close to it. Apparently, the possibility of bond slip with bar pullout contributes to ductility of failure, and its prevention tends to increase the brittleness of response. From Fig. 2 and 3 it is evident that there is a significant size effect and that the size effect agrees relatively well with the size-effect law in Eq. (2).

In Fig. 3, all the observed failure loads for the second series were analyzed. Due to the fact that the specimens of the smallest size exhibited a different failure mode, the results for all the sizes except the smallest one are reanalyzed in Fig. 4. However, the optimal fit by the size-effect curve is found to differ little from that in Fig. 3. It is interesting that the peak loads measured on the smallest specimens agreed quite well with the overall trend of the size effect, even though the failure mode was not completely diagonal shear. This might be due to the fact that the beam depth was only four times the maximum aggregate size, in which case different types of failure mode must blend because the cracking pattern is dominated by the random locations of aggregate pieces.

Since the first series did not involve the largest size of $d = 330$ mm (13 in.), the three middle sizes of the second series are analyzed separately in Fig. 5, which may be compared to Fig. 2. In this case the optimal size-effect curve is somewhat more remote from the linear elastic fracture mechanics asymptote and is somewhat closer to the optimal curve from the first series.

Comparing Fig. 2 to 5 with similar size-effect plots constructed in previous works[2-4] that were based on the test data extracted from the literature, one must note that the width of the scatter band is far narrower for the present tests, as expected. The reason for this is that the specimens in the present tests did satisfy the condition of geometrical similarity and that the size range

272

was considerably broader. This makes it possible to draw stronger conclusions.

IMPLICATION FOR CODE DESIGN FORMULA

At present, the design codes generally ignore the size effect (although some include a mild size effect, the correctness of which is questionable). The present formula for the nominal strength of concrete in diagonal shear, given by ACI 318, reads

$$v_c = \min\left\{ 1.9\sqrt{f_c'} + 2500\rho \frac{V_u d}{M_u}, \quad 3.5\sqrt{f_c'} \right\} \quad (3)$$

where f_c' and v_c are in psi (1 psi = 6895 Pa); ρ is the reinforcement ratio; and M_u is the moment occurring simultaneously with shear force V_u at the cross section considered. In our case, $V_u = P_u/2$ and the moment at the distance d from the supports is $M_u = (a_s - d)P_u/2$. For the present test specimens, $V_u d/M_u = d/(a_s - d) = 0.5$, and then $v_c = 1.222$ MPa (177.2 psi) and 1.212 MPa (175.8 psi) for the first and second series, respectively; a_s is the shear span of the beam (Fig. 1).

Eq. (3) gives the ultimate capacity without any size effect. According to the size-effect law in Eq. (2), it appears that Eq. (3) should be adjusted by multiplying it with the factor $B(1 + \beta)^{-1/2}$, i.e., the nominal strength of concrete in diagonal shear ($v_u = \sigma_N$) should be taken as

$$v_u = Bv_c (1 + \beta)^{-1/2}, \qquad \beta = \frac{d}{d_0} \quad (4)$$

with v_c defined by Eq. (3). For beams of sizes $d > d_c$, where $d_c = (B^2 - 1)d_0$ (which corresponds to $v_u = v_c$), the ACI relation [Eq. (3)] will not meet the required safety margin. For $d < d_c$, the design will be uneconomic. The value of d_c of course depends on the value of B. For the first test series (Fig. 2), $d_c = 355$ mm (14.0 in.), and for the second series (Fig. 3), $d_c = 150$ mm (5.9 in.). Note, however, that we are concerned here with the ultimate loads, while the ACI formula is in fact intended to reflect the diagonal crack-initiation load. Perhaps both Eq. (3) and (4) should be considered. For smaller sizes ($d \leqslant d_c$), Eq. (3) will govern, and for larger sizes, Eq. (4) will govern.

Eq. (3) and (4) represent the necessary adjustment that is closest to the current ACI Building Code. A better formulation involving the size effect was presented in References 2 and 4. Comparisons of the present data with this and other formulations are planned.

For beams with stirrups, the shear capacity due to stirrups (calculated in the usual manner and not subjected to any size-effect correction) must be added to that in Eq. (4), as is the current practice. However, note that the presence of stirrups affects to some extent the carrying capacity (i.e., the nominal strength at failure) due to concrete, as became apparent from the study in Reference 4, but this remains to be explored experimentally. The simple formula obtained in the earlier paper might be used; however, the problem deserves deeper investigation.

To apply Eq. (2) [or Eq. (4)] with the size effect, one needs to determine the brittleness number. In the absence of measurements, this can be done according to one of the following two formulas[7,10,12]

$$\beta = \frac{d}{d_0} = \frac{B_k^2 (\alpha_0)}{c_n^2} \frac{d}{\ell_u} \quad (5)$$

$$\beta = \frac{d}{d_0} = \frac{g (\alpha_0)}{g' (\alpha_0)} \frac{d}{c_f} \quad (6)$$

in which G_f = fracture energy, c_f = effective size of the fracture process zone, E = Young's modulus of elasticity, $\ell_u = EG_f/v_c^2$, $g(\alpha_0)$ = nondimensionalized energy release rate for the relative crack length $\alpha_0 = a_0/d$, where a_0 = length of the part of main crack at failure that is traction-free (i.e., free of bridging stress), and $g'(\alpha)$ = derivative of $g(\alpha)$.

Eq. (5), derived in Reference 7 and discussed in Reference 10, is more accurate for small specimen sizes (near plasticity). On the other hand, Eq. (6), derived in Reference 12, is more accurate for large sizes (near linear elastic fracture mechanics). If these differences are ignored, the size-effect parameters B and d_0 can be estimated approximately as

$$d_0 = \frac{g' (\alpha_0)}{g (\alpha)} c_f, \qquad B = c_n \left(\frac{\ell_u}{g' (\alpha_0)c_f} \right)^{1/2} \quad (7)$$

If B can be estimated from plastic analysis, then [according to Eq. (5)] the length parameter in the size-effect law may be calculated as $d_0 = c_n^2 \ell_u / B^2 g (\alpha_0)$.

However, it is not presently completely clear how Eq. (5) and (6) should be applied in design. Parameters G_f, c_f, and E are material constants that can be deduced from simple experiments; however, a more serious question arises with regard to the meaning of $g(\alpha_0)$. The shape and length of the equivalent linear elastic crack at the moment of diagonal shear failure must be determined, as must how $g(\alpha_0)$ depends on the steel ratio ρ and the shear span a_s/d. These questions require further investigation. Numerical finite element analysis could of course be employed,[13] but even that is of limited value due to limited knowledge of the material laws. In the meantime, a practical alternative might be to develop some empirical equations for the values of B and d_0, from which the brittleness number β would follow.[2-4,14]

The value of parameter d_0, which is required to determine the brittleness number, is no doubt related to some length property of the microstructure of concrete. This might be, at least partially, the maximum aggregate size d_a. However, the length of the effective fracture process zone at failure c_f might be more important; c_f is a material parameter whose value can be obtained from size-effect tests of notched fracture specimens of different sizes.[12,15]

Using previous fracture tests[10] done on a similar concrete, it was estimated[12] that $c_f = 1.7$ mm (0.067 in.). According to the present tests, $d_0 = 95c_f$ (range 2:8, see Fig. 2) for the first series with unanchored bars, and $d_0 = 5.2c_f$ (range 1:16, see Fig. 3) or $d_0 = 39c_f$ (range 2:8, Fig. 5) for the second series with anchored bars. But
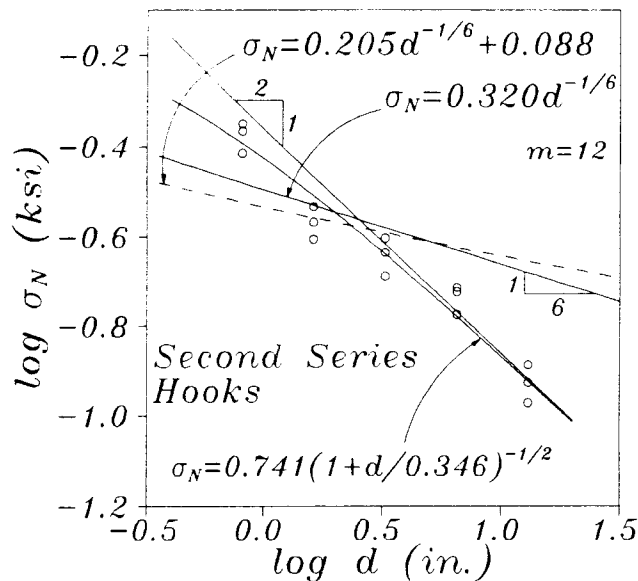
$\sigma_N = 0.205 d^{-1/6} + 0.088$

$\sigma_N = 0.320 d^{-1/6}$

$m = 12$

Second Series Hooks

$\sigma_N = 0.741(1 + d/0.346)^{-1/2}$

Fig. 6—Weibull-type size effect for the second series (1 in. = 25.4 mm, 1 ksi = 6.895 MPa)

these values of d_0 are too scattered to consider as a general property.

Statistical scatter might not be the only reason for these differences of the values of d_0 for different sizes. For example, disregarding the main crack that leads to complete fracture of the beam, there are prepeak cracks which may also have some influence, affecting function $g(\alpha_0)$. The number of these cracks is greater for larger beams,[11,14] which might make function $g(\alpha_0)$ size dependent in effect. Further, for smaller beams, the aggregate interlock on crack[16] and mixed-mode effect[13,17] (crack opening with shear) play a greater role in carrying the load.

One must keep in mind the various abnormalities of the present tests. Due to the need to scrupulously enforce geometric similarity, the steel cover of the largest beams has been uncharacteristically thick at the bottom and thin at the sides. The diameters of the reinforcing bars could not be scaled exactly (which may affect the size effect through bond slip[18]). The steel bars were of high strength. Probably, these aspects should not significantly alter the size-effect results, but this remains to be proven. Finally, the most serious limitation of the present tests is that the concrete was of reduced aggregate size.

In some types of brittle failure, e.g., the Brazilian split-cylinder test, measurements revealed an upper size limit on the validity of the size-effect law in Eq. (2), after which the size effect disappears and there is a transition to a different failure mechanism.[19] The range of applicability of Eq. (2) is probably also limited for the case of diagonal shear, but if such a limit exists, it appears to lie beyond the range 1:16.

The size effect in diagonal shear should be of particular concern for high-strength concrete[1] since the results of Reference 20 showed that the higher strength concrete has a smaller c_f than normal concrete.

WEIBULL-TYPE SIZE EFFECT AND OTHER ASPECTS

It has been widely believed that the size effect in concrete structures can be explained by Weibull-type weakest-link statistical theory. This theory, however, ignores the large stress redistribution that happens between the crack initiation load and the ultimate load. This redistribution makes Weibull's statistical strength theory inapplicable to concrete structures,[7,8,21] unless the failure occurs at the initiation of cracking (strictly speaking, at the initiation of *macroscopic* cracking, since microcracks can and do exist at lower loads).

The test results of the second series in Fig. 6 make it possible to check the applicability of Weibull-type theory to diagonal shear. This theory yields the most severe size effect when the threshold of strength distribution σ^u is taken as $\sigma_u = 0$. In that case, the theory predicts the plot of log σ_N versus log d to be a straight line of slope $-\frac{1}{6}$ if there is two-dimensional similarity and the value of Weibull modulus m is taken according to uniaxial test results for concrete (which typically give $m = 12$). Fig. 6 clearly shows how the Weibull theory disagrees with the present tests, giving too weak a size effect in the large size range. So far the evidence against the application of Weibull theory to structures with large fracture growth prior to failure has been theoretical,[7,8] and this seems to be the first experimental evidence.

If the Weibull threshold σ_u is taken as $\sigma_u = 0.5\ v_c$ [Eq. (3)], then the Weibull theory (with $m = 12$) predicts the dashed curve, which disagrees with the present tests even more. One could also adjust the Weibull modulus m to yield an optimal fit of the present tests, but such a value of m would disagree with direct tension tests. Nonlinear regression of the equation $\sigma_N = A_d^{-2\,m} + \sigma_u$ yields $m = 3.15$, $\sigma_u = 0.52$ MPa (75.4 psi), and $A' = 0.199$ MPa $\cdot$ m$^{2/m}$ [297 psi (in.)$^{2/m}$] as the optimum fit. It should be added that if there is size effect in σ_N at crack initiation, it may have to be explained by a Weibull-type theory, since the size-effect law in Eq. (2) does not apply to σ_N crack initiation.[14]

For two- and three-dimensional similarity, Weibull theory with zero threshold and $m = 12$ indicates that σ_N should be proportional to $d^{-1/6}$ and $d^{-1/4}$, respectively. Factor $d^{-1/4}$ was proposed by Kani[11] on the basis of his experiments. Shioya et al. (see Reference 16) proposed the factor $[(d/d_1)^{-1/4} - 1]$ where $d_1 = $ constant. Factor $d^{-1/4}$ was also suggested by Gustafsson and Hillerborg,[8] based, however, not on statistics but on approximating their calculation results according to the fictitious crack model for the range of $0.3 < d/\ell_0 < 5$ (where $\ell_0 = EG_f/f_t$ and f_t is tensile strength). A similar size-effect trend, based on nonlinear fracture mechanics calculations, was obtained by Jenq and Shah.[17] The aforementioned authors[17] consider the effect of thickness to be negligible, as indicated by Kani's tests (which contradict Weibull theory). Keep in mind though, that when the size-effect range is too limited or the scatter of test data is too large, different size-effect laws can fit the available test data equally well.

After the review of this paper,[17] Walraven published a series of diagonal shear tests.[14] He concluded that the size-effect law in Eq. (2) can be used for diagonal shear of beams with different ratios of shear span to beam depth (although for $a_s/d = 1$ the failure was completely different than diagonal shear). This reinforces the conclusions of this study.

Although concrete is not a deterministic material, a statistical size effect should nevertheless exist.[9] The question is how significant it is, and how to calculate it. This question was recently studied by Bažant and Xi,[22] who showed that for materials with a large fracture process zone in which a large crack grows in a stable manner prior to ultimate load, a nonlocal generalization of Weibull theory is required. In this theory, the failure probability of the material at a certain point does not depend on the stress at that point but on the average of stress (or strain) from a certain neighborhood of the point. This theory leads to the following formula

$$\sigma_N = Bf_u \, (\beta^{2n/m} + \beta)^{-1/2}, \qquad \beta = \frac{d}{d_0} \qquad (8)$$

where m = Weibull modulus ($m \approx 12$) and n = number of dimensions ($n = 2$ for two-dimensional similarity and $n = 3$ for three-dimensional similarity). Eq. (2) is obtained as the deterministic limit of Eq. (8) for $m \to \infty$. In the plot of log σ_N versus log β, Eq. (8) describes a smooth transition from a straight line of slope $-n/m$ (rather than from a horizontal line) to a straight line of slope $-\frac{1}{2}$. In practice, the difference between Eq. (2) and (9) becomes significant only if the size range is very broad and includes very small sizes. As for the present test results, Eq. (8) fits them better, but only slightly better, than does Eq. (2).

It has been proposed that the classical Weibull-type theory of size effect should apply to the loads at crack initiation. Strictly speaking, that would be exactly true only if upon reaching the strength limit of the material, the cracks formed instantly. In reality, they form gradually; before any microcrack is fully formed, the stress must localize. The localization inevitably causes some size effect of deterministic type, even for the crack-initiation loads. It is unclear whether this size effect, superimposed on a statistical size effect, is really negligible for practical purposes.

CONCLUSIONS

1. The diagonal shear failure exhibits a strong size effect of fracture mechanics type, due to differences in the stored energy that can be released to drive the failure propagation.

2. The present test results are in good agreement with the size-effect law proposed in Reference 6 [Eq. (2)].

3. Prevention of bond slip of bars by providing anchorage at the ends increases the brittleness number.

4. Application of Weibull's (weakest-link) statistical failure theory to diagonal shear failure is disproved by the results of the test series with anchored bars.

5. Since for the ultimate load there is a strong size effect, while for the first diagonal crack-initiation load the size effect is small or negligible, imposition of a certain margin of safety against the crack-initiation load does not insure a uniform margin of safety against the ultimate load. Consequently, a requirement based on the ultimate load has to be introduced into design codes, which means the size effect (of fracture mechanics type) has to be considered. (However, the present criterion based on the diagonal crack-initiation load, involving little or no size effect, should perhaps be retained as a second design requirement, to insure serviceability; it might govern for small sizes, while the ultimate load criterion with the size-effect law would govern for large sizes.)

REFERENCES

1. Thorenfeldt, E., and Drangsholt, G., "Shear Capacity of Reinforced High Strength Concrete Beams," *High Strength Concrete—Second International Symposium*, SP-121, American Concrete Institute, Detroit, 1990, pp. 129-154.

2. Bažant, Zdeněk P. and Kim, Jin-Keun, "Size Effect in Shear Failure of Longitudinally Reinforced Beams," ACI JOURNAL, *Proceedings* V. 81, No. 5, Sept.-Oct. 1984, pp. 456-468. Also, Discussion, ACI JOURNAL, *Proceedings* V. 82, No. 4, July-Aug. 1985, pp. 579-583.

3. Bažant, Zdeněk P., and Cao, Zhiping, "Size Effect of Shear Failure in Prestressed Concrete Beams," ACI JOURNAL. *Proceedings* V. 83, No. 2, Mar.-Apr, 1986, pp. 260-268.

4. Bažant, Zdeněk P., and Sun, Hsu-Huei, "Size Effect in Diagonal Shear Failure: Influence of Aggregate Size and Stirrups," *ACI Materials Journal*, V. 84, No. 4, July-Aug. 1987, pp. 259-272.

5. Reinhardt, H. W., "Similitude of Brittle Fracture of Structural Concrete," *Advanced Mechanics of Reinforced Concrete*, IABSE Colloquium, Delft, 1981, pp. 175-184.

6. Bažant, Z. P., "Size Effect in Blunt Fracture: Concrete, Rock, Metal," *Journal of Engineering Mechanics*, ASCE, V. 110, EM4, 1984, pp. 518-535.

7. Bažant, Z. P., "Fracture Energy of Heterogeneous Material and Similitude," *Proceedings*, RILEM-SEM International Conference on Fracture of Concrete and Rock (Houston, June 1987), Springer-Verlag, New York, 1989, pp. 229-241.

8. Gustafsson, Per Johan, and Hillerborg, Arne, "Sensitivity in Shear Strength of Longitudinally Reinforced Concrete Beams to Fracture Energy of Concrete," *ACI Structural Journal*, V. 85, No. 3, May-June 1988, pp. 286-294.

9. Carpinteri, A., "Decrease of Apparent Tensile and Bending Strength with Specimen Size: Two Different Explanations Based on Fracture Mechanics," *International Journal of Solids and Structures*, V. 25, No. 4, 1989, pp. 407-429.

10. Bažant, Zdeněk P., and Pfeiffer, Philip A., "Determination of Fracture Energy from Size Effect and Brittleness Number," *ACI Materials Journal*, V. 84, No. 6, Nov.-Dec. 1987, pp. 463-480.

11. Kani, G. N. J., "How Safe Are Our Large Reinforced Concrete Beams?" ACI JOURNAL, *Proceedings* V. 64, No. 3, Mar. 1967, pp. 128-141.

12. Bažant, Z. P., and Kazemi, M. T., "Determination of Fracture Energy, Process Zone Length and Brittleness Number from Size Effect, with Application to Rock and Concrete," *International Journal of Fracture*, V. 44, 1990, pp. 111-131.

13. Saouma, V. E., and Ingraffea, A. R., "Fracture Mechanics Analysis of Discrete Cracks," *Advanced Mechanics of Reinforced Concrete*, IABSE Colloquium, Delft, 1981. pp. 413-436.

14. Walraven, J., "Scale Effects in Beams with Unreinforced Webs, Loaded in Shear," *Progress in Concrete Research*, Annual Report, Delft University of Technology, The Netherlands, V. 1, 1990, pp. 101-112.

15. Bažant, Z. P., and Kazemi, M. T., "Size Effect in Fracture of Ceramics and Its Use to Determine Fracture Energy and Effective Process Zone Length," *Report* No. 89-6/498s, Center for Advanced Cement-Based Materials, Northwestern University, Evanston, 1989. Also, *Journal of the American Ceramics Society*, V. 73, No. 7, 1990, pp. 1841-1853.

16. Shioya, T.; Iguro, M.; Nojiri, Y.; Akiayama, H.; and Okada, T., "Shear Strength of Large Reinforced Concrete Beams," *Fracture Mechanics: Application to Concrete*, SP-118, American Concrete Institute, Detroit, 1989, pp. 259-279.

17. Jenq, Y. S., and Shah, S. P., "Shear Resistance of Reinforced Concrete Beams—A Fracture Mechanics Approach," *Fracture Mechanics: Application to Concrete*, SP-118, American Concrete Institute, Detroit, 1989, pp. 237-258.

18. Soroushian, Parviz, and Choi, Ki-Bong, "Local Bond of Deformed Bars with Different Diameters in Confined Concrete," *ACI Structural Journal*, V. 86, No. 2, Mar.-Apr. 1989, pp. 217-222.

19. Bažant, Z. P.; Kazemi, M. T.; Hasegawa, T.; Mazars, J.; and Saouridis, C., "Size Effect in Brazilian Split-Cylinder Tests: 1. Measurements and Fracture Analysis," *Report* No. 90-5/618s, Center for Advanced Cement-Based Materials, Northwestern University, Evanston, 1990.

20. Gettu, R.; Bažant, Z. P.; and Karr, M. E., "Fracture Properties of High Strength Concrete," *Report* No. 89-10/B627f, Center for Advanced Cement-Based Materials, Northwestern University, Evanston, 1989. Also, *ACI Materials Journal*, V. 87, No. 6, Nov.-Dec. 1990, pp. 608-618.

21. Bažant, Z. P.; Xi, Y.; and Reid, S. G., "Statistical Size Effect in Quasibrittle Structures: Part 1. Is Weibull Theory Applicable?" *Report* No. 90-5/616s(1), Center for Advanced Cement-Based Materials, Northwestern University, Evanston, 1990.

22. Bažant, Z. P., and Xi, Y., "Statistical Size Effect in Quasibrittle Structures: Part II. Nonlocal Theory," *Report* No. 90-5/616s (II), Center for Advanced Cement-Based Materials, Northwestern University, Evanston, 1990.